

# Improving the Van Bavel-Hillel model for soil evaporation in grasslands by introducing vegetation coverage resistance

Lanjuan Li<sup>1</sup>, Xiaoyu Song<sup>1\*</sup>, Lu Xia<sup>2</sup>, Fanning Dang<sup>1</sup>, Xinkai Zhao<sup>1</sup>,  
Pengfei Meng<sup>1</sup>, Dan Feng<sup>3</sup>, Huaiyou Li<sup>4</sup>

(1. State Key Laboratory of Eco-hydraulics in Northwest Arid Region of China, Xi'an University of Technology, Xi'an 710048, China;

2. College of Resources and Environment, Shanxi Agricultural University, Jinzhong 030801, Shanxi, China;

3. Lantian Water Conservancy and Soil and Water Conservation Workstation, Xi'an 710500, China;

4. Xifeng Experimental Station on Soil and Water Conservation of Yellow River Conservancy Committee, Qingyang, 745000, Gansu, China)

**Abstract:** Modeling the soil evaporation under vegetation conditions is of theoretical and practical significance for water resources management in the Loess Plateau. In this study, a three-year field experiment was conducted in a bare land and three grasslands to measure soil evaporation using micro-lysimeters. The Van Bavel-Hillel model was then validated in the bare land. Based on this, the vegetation coverage resistance was proposed to reflect the comprehensive effects of vegetation, and it was applied into the Van Bavel-Hillel model to improve the model's applicability under vegetation conditions. The results showed that the Van Bavel-Hillel model was effective in simulating evaporation from bare land, and the application of validated soil surface resistance and vegetation coverage resistance can make it perform well in the evaporation simulation in all studied grasslands. The obtained vegetation coverage resistances decreased linearly with the increase of soil moisture contents in all three grasslands, and the decreasing rates were similar in the *M. sativa* and *P. giganteum* plots, which were higher than that in the *I. cylindrica* plot. Soil surface resistances ranged between 533.4-746.5, 767.4-1154.7, and 133.4-1334.5 s/m in the *I. cylindrica*, *M. sativa*, and *P. giganteum* plots, respectively, and all showed the characteristics of first increasing and then decreasing during the growing season. When compared with natural grassland, *M. sativa* increased the soil surface resistance in all months, while *P. giganteum* reduced it in the early growing season, but increased it in the middle and late growing season. This research proposes a new idea for the simulation of soil evaporation under vegetated conditions, and provides a basic reference for water resources management in the vegetation restoration of the Loess Plateau.

**Keywords:** soil evaporation, Van Bavel-Hillel model, evaporation resistance, grassland, water management

**DOI:** 10.25165/ijabe.20251801.7081

**Citation:** Li L J, Song X Y, Xia L, Dang F N, Zhao X K, Meng P F, et al. Improving the Van Bavel-Hillel model for soil evaporation in grasslands by introducing vegetation coverage resistance. Int J Agric & Biol Eng, 2025; 18(1): 191-198.

## 1 Introduction

Soil evaporation ( $E$ ) plays an important role in the water cycle and energy balance in ecosystems, and its occurrence processes and quantitative characteristics will directly affect the water management and regulation in the field<sup>[1,2]</sup>.  $E$  is a kind of non-productive water loss since it does not directly participate in the vegetation physiological processes<sup>[3]</sup>. Therefore, accurately quantifying  $E$ , and based on which, putting forward specific measures to reduce this part of water consumption, is of great

significance to deepen the understanding of regional hydrological processes, utilization of water resources, and the improvement of water use efficiencies<sup>[4,5]</sup>.

$E$  is controlled by meteorological conditions (e.g., solar radiation, temperature, and wind speed) and water supply conditions (mainly soil water supply)<sup>[6]</sup>. Previous studies have shown that the introduction of vegetation tended to greatly block solar radiation or increase the resistance of soil water movement<sup>[7,8]</sup>, and eventually lead to a decrease of  $E$ <sup>[4,6]</sup>. Based on the above understanding, many empirical or semi-empirical models have been developed, and have undoubtedly greatly facilitated the calculation of  $E$  under specific vegetation conditions<sup>[9-12]</sup>. However, their applicability always varied geographically<sup>[13]</sup>, as a result of which the understanding of  $E$  calculation is still insufficient to date. Affected by the heterogeneity of climatic and underlying conditions, influence degrees of meteorological and soil moisture conditions on  $E$  are often not fixed, and always differ greatly in various ecosystems<sup>[6,14,15]</sup>. In fact, there is always no significant relationship between  $E$  and meteorological factors or soil water supply<sup>[4]</sup>. Therefore, it is necessary to develop more universal models to further clarify the role of meteorological conditions and soil moisture. However, when this type of model is applied, the acquisition of the evaporation resistance is an important limiting factor. Taking the widely used Van Bavel-Hillel model as an example, although it can simulate soil evaporation in bare land well, the calibration of its parameters

**Received date:** 2021-09-24 **Accepted date:** 2024-09-17

**Biographies:** Lanjuan Li, PhD candidate, research interest: ecohydrological process and water resources management, Email: [li\\_lanjuan@126.com](mailto:li_lanjuan@126.com); Lu Xia, PhD, Associate professor, research interest: hydrology and water resources, Email: [xialuxiaochen@163.com](mailto:xialuxiaochen@163.com); Fanning Dang, PhD, Professor, research interest: numerical analysis of hydraulic structures and geotechnical engineering, Email: [dangfn@mail.xaut.edu.cn](mailto:dangfn@mail.xaut.edu.cn); Xinkai Zhao, PhD candidate, research interest: soil and water conservation and its environmental effects, Email: [xinkaizhao@126.com](mailto:xinkaizhao@126.com); Pengfei Meng, PhD candidate, research interest: hydrology and water resources, Email: [1010334173@qq.com](mailto:1010334173@qq.com); Dan Feng, MD, research interest: soil and water conservation and its environmental effects, Email: [934326127@qq.com](mailto:934326127@qq.com); Huaiyou Li, BD, Professor, research interest: soil and water conservation and desertification control, Email: [153120111@qq.com](mailto:153120111@qq.com).

\*Corresponding author: Xiaoyu Song, PhD, Professor, research interest: hydrology and water resources. Xi'an University of Technology, No.5, Jinhua South Road, Xi'an 710048, Shaanxi, China. Tel: +86-13572593963, Email: [songxy@xaut.edu.cn](mailto:songxy@xaut.edu.cn).

requires a lot of field experiments<sup>[9]</sup>. When the impact of vegetation is taken into account, its applicability will also be limited, which further demonstrates the necessity of conducting in-depth research to improve the applicability of such models.

The Loess Plateau ( $6.4 \times 10^5$  km<sup>2</sup>) situated in northwest China is one of the areas with the most serious soil erosion in the world<sup>[16]</sup>. To mitigate soil erosion and land degradation, the Chinese government launched the Grain to Green project in 1999, and has converted 16 000 km<sup>2</sup> of slope cropland to planted vegetation<sup>[17]</sup>. These planted vegetations, including afforestation and grass, indeed significantly altered hydrological processes, and thus greatly reduced runoff generation and soil losses<sup>[17]</sup>. However, they simultaneously bring some negative effects on regional water resources and ecology, such as the reduction of runoff available and the formation of soil desiccation<sup>[18,19]</sup>. Among the planted vegetation, grass species were highly recommended since they always consumed less water than trees, and were more likely to achieve the trade-off between soil erosion mitigation and water resources limitation<sup>[18]</sup>. In fact, numerous studies have been conducted to study the transpiration characteristics in grassland ecosystems, while limited research has involved their *E* processes<sup>[4,20]</sup>. Moreover, research comparing the different effect mechanisms of natural and planted grasslands on *E* is lacking. However, such information provides the basis for developing policies for grassland conservation and water resources management. Therefore, it also needs to be taken seriously and studied in depth.

This study was carried out in these contexts. A three-year field experiment was conducted in an abandoned bare land and three typical grasslands (one natural and two planted grasslands) in the semi-arid Loess Plateau, to observe their *E* processes and to measure their related influencing factors (i.e., meteorological factors and soil moisture contents). The main objectives of this study were to: 1) investigate the effect of soil water conditions on *E* characteristics; 2) establish the calculation formula of *E* under vegetation conditions; and 3) compare differences of soil evaporation resistances between natural and planted grasslands. The results of the study will enhance our comprehension of the *E* processes in typical grasslands, and provide theoretical and practical guidance for grass species selection and water resources management in the Loess Plateau.

## 2 Materials and methods

### 2.1 Study area and experimental plots

Field experiments were conducted in Nanxiaohegou Basin ( $35^{\circ}41' - 35^{\circ}44' \text{N}$ ,  $107^{\circ}30' - 107^{\circ}37' \text{E}$ ; altitude: 1058-1450 m), a typical small-scale basin (36.5 km<sup>2</sup>) selected by the Yellow River Conservancy Committee, China, which is situated in the central Loess Plateau. The study area experiences a warm temperate continental climate, with average annual precipitation and daily temperature reaching 535.9 mm and 8.7°C, respectively<sup>[4]</sup>. Intra-annual precipitation varies greatly in each month, and above 65.0% of the annual precipitation occurred in June-September as heavy rainstorms. The area has a single geology characteristic, with almost all of the basin being covered by the loess soil (more than 200 m thick), which is prone to water erosion<sup>[21]</sup>. The dominant land use types include grasslands (*Imperata cylindrica*, *Medicago sativa*, *Pennisetum giganteum*, and *Celosia cristata*), shrublands (*Hippophae rhamnoides* and *Sophora viciifolia*), forestlands (*Platycladus orientalis*, *Robinia pseudoacacia*, *Pinus tabuliformis*, and *Prunus armeniaca*), and abandoned bare land, and the growing season for

most vegetation species is from mid-April to mid-October.

After field surveys, a natural grassland (the *I. cylindrica* plot) and two planted grasslands (the *M. sativa* and *P. giganteum* plots) were selected as experimental plots since they are typical and widely distributed in the study area. In addition, an abandoned plot of bare land was also selected as the control group, to reveal different effects of each grass species on *E*. These plots were close to each other and had similar environmental conditions. *I. cylindrica* and *P. giganteum* are perennial gramineous species, whereas *M. sativa* is a perennial leguminous species. *M. sativa* and *P. giganteum* were planted in late April 2014 to increase grass production. Between them, *M. sativa* was sown in drills, with a sowing density of 2.0 kg/hm<sup>2</sup> and a row space of 30 cm, while *P. giganteum* was planted using the stem segment cottage method, with a planting distance of 20 cm and a row space of 50 cm. During growing seasons, no management measures or harvesting were implemented, in order to prevent rainstorm-induced soil erosion. More detailed information about the experimental plots is listed in Table 1.

**Table 1 Detailed information about the vegetation and topography of experimental plots**

Plots	Plant height/m	Coverage degree	Altitude/m	Terrain	Slope position	Slope grade/°
<i>I. cylindrica</i>	21.4±4.6	0.91	1214	Terrace of sloping field	Middle	11
<i>M. sativa</i>	44.9±8.1	0.75	1189	Terrace of sloping field	Middle	32
<i>P. giganteum</i>	224.6±21.8	0.84	1221	Terrace of valley	Down	0

### 2.2 Measurements and observations

The experimental periods lasted for three consecutive growing seasons (April 15th-October 15th in 2015-2017). The vegetation height was measured using a tape (accuracy 1 mm), with a time interval of approximately one week, and with nine replicates. As the soil evaporation mainly consumes the water from shallow soil<sup>[2,22]</sup>, the soil properties in this study were mainly determined at surface layers (0-5 cm) soon before the first growing seasons. Soil water retention curves and soil texture were measured once by a centrifuge system (Kokusan Ltd., H-1400p F, Japan) and a laser sizer (Malvern Instruments Ltd., Malvern Master Sizer 2000, UK), respectively. Soil organic matter was determined three times by the potassium dichromate methods<sup>[4]</sup>. The bulk density, field water capacity, and saturated water content were determined using the cutting ring method<sup>[16]</sup>, with three replicates. Detailed information about the soil properties is listed in Table 2.

**Table 2 Detailed information of soil properties in the experimental plots**

Plots	SOM/ %	$\alpha$ / cm <sup>-1</sup>	$n$	$\theta_f$ / cm <sup>3</sup> ·cm <sup>-3</sup>	$\theta_s$ / cm <sup>3</sup> ·cm <sup>-3</sup>	BD	Particle size distribution/%		
							Clay	Silt	Sand
<i>I. cylindrica</i>	1.48±0.06	0.0141	1.2019	0.328±0.01	0.489±0.02	1.26±0.03	9.7	74.6	15.7
<i>P. giganteum</i>	0.88±0.04	0.0098	1.2644	0.339±0.02	0.502±0.03	1.20±0.01	8.2	78.3	13.5
<i>M. sativa</i>	1.04±0.02	0.0277	1.2291	0.332±0.01	0.484±0.03	1.24±0.02	4.3	86.0	9.7

Notes: SOM denotes soil organic matter;  $\alpha$  and  $n$  are reciprocal of inlet air suction and the parameter of pore size distribution in the van Genuchten-Mualem model<sup>[23,24]</sup>, respectively.  $\theta_f$ ,  $\theta_s$ , and BD are field water capacity (cm<sup>3</sup>/cm<sup>3</sup>), saturated soil moisture content, and bulk density, respectively. Particle size distribution is classified according to soil textural classes of United States Department of Agriculture (USDA).

Three meteorological stations (Spectrum Technologies, Inc., Watchdog 2000 series, USA) were set up to record hourly

meteorological data, including precipitation, air temperature, wind speed, solar radiation, and relative humidity at height of 2 m. Hourly data were then converted to daily data for later analysis. The frequency of measuring soil evaporation was set to once every 1-7 d according to weather conditions. A total of nine micro-lysimeters (25 cm in height and 16 cm in diameter, three for each plot) were randomly installed in the selected plots to monitor  $E$  (accuracy 0.01 g). It should be noted that the spacing between grasses in each plot was relatively close (30-50 cm in the planted grasslands), and their canopy increased rapidly, quickly resulting in a high level of coverage (Table 1). Therefore, the lysimeters are closely affected by shading and root water use, making them very representative for the studied plots. Soil moisture content and soil temperature were measured using two tubular time domain reflectometers (Aozuo Ecology Instrumentation Ltd., Trime-Pico TDR, China). The measuring time was consistent with the observation of the soil moisture contents, and the measurement depths were set as 0, 10, 20, 30, and 40 cm soil layers, respectively, considering that  $E$  is mainly affected by the moisture content of surface soil<sup>[2,22]</sup>. As the measurement of 0 cm layers (surface layers) was difficult to operate, these values were measured from the layers slightly lower than the soil surface (about 1 cm below). Multiple readings of observations (three for  $E$ , and two for soil moisture content and soil temperature) were averaged to represent the average level of each plot and soil depth.

### 2.3 The model of soil evaporation

#### 2.3.1 The model of soil evaporation from the bare land

The numerical simulation model developed by Van Bavel and Hillel<sup>[9,25]</sup> has the advantages of having a simple theoretical basis and easy parameter acquisition, and has therefore been successfully applied in  $E$  calculation with straw coverage or gravel mulching<sup>[22,26]</sup>. However, to our knowledge, it has not been proven to be effective under vegetated conditions. Therefore, its application deserves further research. The basic form of the Van Bavel-Hillel model for bare soil is as follows<sup>[25,22]</sup>:

$$E_b = \frac{H_{vs} - H_{va}}{r_a + r_s} \quad (1)$$

where,  $E_b$  is the soil evaporation rate of the bare land, mm/s;  $H_{vs}$  is the absolute air humidity on the soil surface, kg/m<sup>3</sup>;  $H_{va}$  is air humidity, kg/m<sup>3</sup>;  $r_a$  is the aerodynamic resistance of water vapor when entering from the soil surface to the atmosphere, s/m;  $r_s$  is the soil surface resistance of water vapor in soil pores, s/m.  $H_{vs}$ ,  $H_{va}$ ,  $r_a$ , and  $r_s$  can be calculated as following<sup>[9,27,28]</sup>:

$$H_{vs} = H_{vss} \cdot \exp\left(\frac{\phi g}{R(T_s + 273.16)}\right) \quad (2)$$

where,  $\phi$  is the water potential of the surface soil, m, which could be obtained based on the measured soil moisture content and soil water retention curve;  $g$  is the gravitational acceleration, 9.8 m/s<sup>2</sup>;  $R$  is the universal or ideal gas constant, 8.314 J/(mol·K);  $T_s$  is the soil surface temperature, °C;  $H_{vss}$  is the saturated humidity of the soil surface, kg/m<sup>3</sup>, which can be calculated as:

$$H_{vss} = \frac{1.323 \exp\left(\frac{17.27T_s}{T_s + 237.3}\right)}{T_s + 273.16} \quad (3)$$

In Equation (1), the parameter  $H_{va}$  can be calculated as:

$$H_{va} = \frac{2.185}{273.16 + T_a} \cdot e_a \quad (4)$$

where,  $T_a$  is the air temperature, °C;  $e_a$  is the actual air vapor pressure, kpa, which can be calculated as:

$$e_a = \frac{RH}{100} 0.6108 \exp\left(\frac{17.27T_a}{T_a + 237.3}\right) \quad (5)$$

where,  $RH$  is the average relative humidity, %;  $T_a$  is the air temperature, °C.

$r_a$  in Equation (1) can be calculated as:

$$r_a = \frac{1}{uk^2} \cdot \ln\left(\frac{Z_{ref} - d + Z_H}{Z_H}\right) \cdot \ln\left(\frac{Z_{ref} - d + Z_m}{Z_m}\right) \quad (6)$$

where,  $u$  is the measured wind speed, m/s;  $k$  is the Karman constant with a value of 0.41;  $Z_{ref}$  is the reference height for measuring air temperature and wind speed, 2 m;  $Z_H$  and  $Z_m$  are surface roughness for heat flux and momentum flux, respectively, m;  $d$  is the zero plane displacement, m.  $Z_H$ ,  $Z_m$ , and  $d$  can be calculated using the following equations<sup>[22]</sup>:

$$Z_H = 0.1Z_m \quad (7)$$

$$Z_m = 0.123h_p \quad (8)$$

$$d = 0.67h_p \quad (9)$$

where,  $h_p$  is the measured height of vegetation, m, with a value of 0 for the bare land.

$r_s$  in Equation (1) can be calculated as:

$$r_s = \begin{cases} 3.5 \left(\frac{\theta_v}{\theta_s}\right)^{2.3} + 33.5, & \frac{\theta_v}{\theta_s} > 0.45 \\ -805 + 4140(\theta_s - \theta_v), & \frac{\theta_v}{\theta_s} \leq 0.45 \end{cases} \quad (10)$$

where,  $\theta_s$  and  $\theta_v$  are saturated surface soil moisture content and observed surface soil moisture content, respectively, cm<sup>3</sup>/cm<sup>3</sup>.

Based on the derivation processes above, the calculation equations of soil evaporation rate could be eventually expressed as follows:

$$E_b = \frac{\exp\left(\frac{\phi g}{R(T_s + 273.16)}\right) \frac{1.323 \exp\left(\frac{17.27T_s}{T_s + 237.3}\right)}{T_s + 273.16} - \frac{RH}{100} \frac{1.323 \exp\left(\frac{17.27}{T_a + 237.3}\right)}{T_a + 273.16}}{r_a + r_s} \quad (11)$$

#### 2.3.2 The model of soil evaporation under vegetation conditions

The Van Bavel-Hillel model has not been used under vegetation conditions, but has been successfully applied in soils with straw coverage or gravel mulching<sup>[22,26]</sup>. In these studies, the effects of straw or gravel were reflected by a resistance parameter. With reference to this approach, the effects of vegetation into a vegetation coverage resistance were considered, and therefore modified the Van Bavel-Hillel model as follows:

$$E_v = \frac{H_{vs} - H_{va}}{r_a + r_s + r_v} \quad (12)$$

where,  $E_v$  is the soil evaporation rate under vegetation conditions, mm/s;  $r_v$  is the newly introduced vegetation coverage resistance, s/m, which was hypothesized to reflect the comprehensive influence of vegetation on  $E$ .

#### 2.3.3 Acquisition of vegetation coverage resistance and soil surface resistance

Numerous studies have shown that when the soil moisture content exceeds a threshold, there is sufficient water in the soil pores, and the status of the water supply from the soil is not destroyed (the soil surface resistance is considered to be zero)<sup>[11,12]</sup>. At this time,  $E$  is mainly controlled by meteorological factors and vegetation effects. Therefore, measured  $E$  under such conditions

could be used to derive the vegetation coverage resistance. According to the modified Van Bavel-Hillel model, Equation (12), the calculation formula of vegetation coverage resistance could be expressed as follows:

$$r_v = \frac{H_{vs} - H_{va}}{E_v} - r_a \quad (13)$$

After obtaining vegetation coverage resistance, the soil surface resistance could be obtained using the measured  $E$  under conditions of soil moisture content lower than the soil moisture content threshold. The calculation equation is as follows:

$$r_s = \frac{H_{vs} - H_{va}}{E_v} - r_a - r_v \quad (14)$$

### 2.4 Model calibration and validation

In this study, the coefficient of consistency ( $C_c$ ) and root mean square error (RMSE) were adopted to evaluate the accuracy of the simulation, and their calculation equations are as follows<sup>[29]</sup>:

$$C_c = 1 - \frac{\sum_{i=1}^n (S_i - O_i)^2}{\sum_{i=1}^n (|S_i - O_{avg}| + |O_i - O_{avg}|)^2} \quad (15)$$

$$RMSE = \sqrt{\frac{1}{n} \sum_{i=1}^n (S_i - O_i)^2} \quad (16)$$

where,  $S_i$  and  $O_i$  are simulated and observed values for the  $i$ th sample, respectively;  $O_{avg}$  is the average observed values;  $n$  is the number of samples. The value of  $C_c$  is distributed between 0 and 1.0, and the closer its value is to 1.0, the better the simulation effect obtained. It is generally considered that a value of  $C_c$  greater than 0.8 indicates good simulation results<sup>[29]</sup>. For RMSE, lower values show better simulation results.

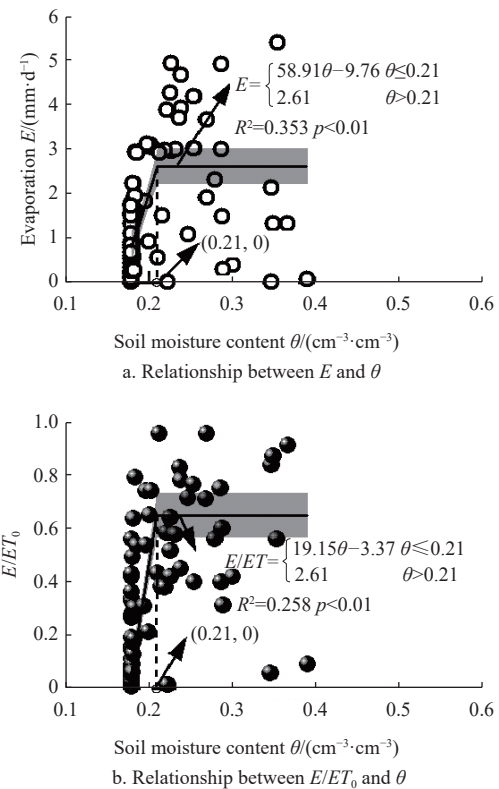
## 3 Results

### 3.1 Effects of soil moisture conditions on soil evaporation

Changes of  $E$  with soil moisture content may exhibit various patterns, such as linear and nonlinear patterns<sup>[30,31]</sup>. To eliminate the influence of vegetation, measured  $E$  of the bare land was used to analyze its relationship with soil moisture contents. As numerous studies have suggested that the use of surface soil moisture content would get better results in  $E$  simulation<sup>[2,22]</sup>, the surface soil moisture content was used in this study for later analysis. Meanwhile, the relative  $E$  (defined as  $E/ET_0$ <sup>[12]</sup>;  $ET_0$  is the reference crop evapotranspiration calculated by the Penman-Monteith formula<sup>[9]</sup>) was also used to eliminate the influence of meteorological factors. Based on the related research<sup>[22]</sup>, this study chose a piecewise function to describe the relationships between  $E$ ,  $E/ET_0$ , and soil moisture content since they exhibited higher coefficients of determination and had passed the significance test (Figure 1).

It can be seen that both  $E$  and  $E/ET_0$  showed piecewise characteristics with changes of soil moisture ( $p < 0.01$ ). According to related studies<sup>[11,22]</sup>, the 60% field water capacity ( $0.210 \text{ cm}^3/\text{cm}^3$  for the bare land) was recognized as the threshold of two stages in this study.  $E$  and  $E/ET_0$  increased linearly and rapidly with the increase of soil moisture when the soil was relatively dryer. However, when the soil moisture exceeded the threshold,  $E$  and  $E/ET_0$  showed little variations with it. Notably,  $E$  and  $E/ET_0$  were relatively scattered when the soil moisture content was higher, which may be due to the replacement of soil moisture content by the average soil moisture content in the analysis. The results above indicated that the 60%

field water capacity was indeed an effective soil moisture threshold to divide different stages of  $E$  in the bare land, which may provide the basis for calculating  $E$  in the studied grasslands.



Note: As the observation intervals are not fixed (1-7 d), the soil evaporation and soil moisture content used in the figures are the average daily values during each observation period.

Figure 1 Relationships between soil evaporation, relative soil evaporation, and soil moisture content in the bare land

### 3.2 Simulation results of soil evaporation from the bare land

The basic form of the Van Bavel-Hillel model, Equation (1), and related parameters were adopted to simulate  $E$  from the bare land during three experimental periods, and the measured  $E$  was used to verify the accuracy of the simulation, as shown in Figure 2. It was evident that RMSE was 2.732, 2.302, and 2.405 mm during years 2015, 2016, and 2017, and corresponding  $C_c$  was as high as 0.930, 0.934, and 0.931, respectively. Such results showed that the simulated  $E$  agreed well with measured ones, indicating that the Van Bavel-Hillel model was effective in simulating  $E$  from the bare land, which also implied that the basic form of the model could be used to deduce related soil evaporation resistances under vegetation conditions.

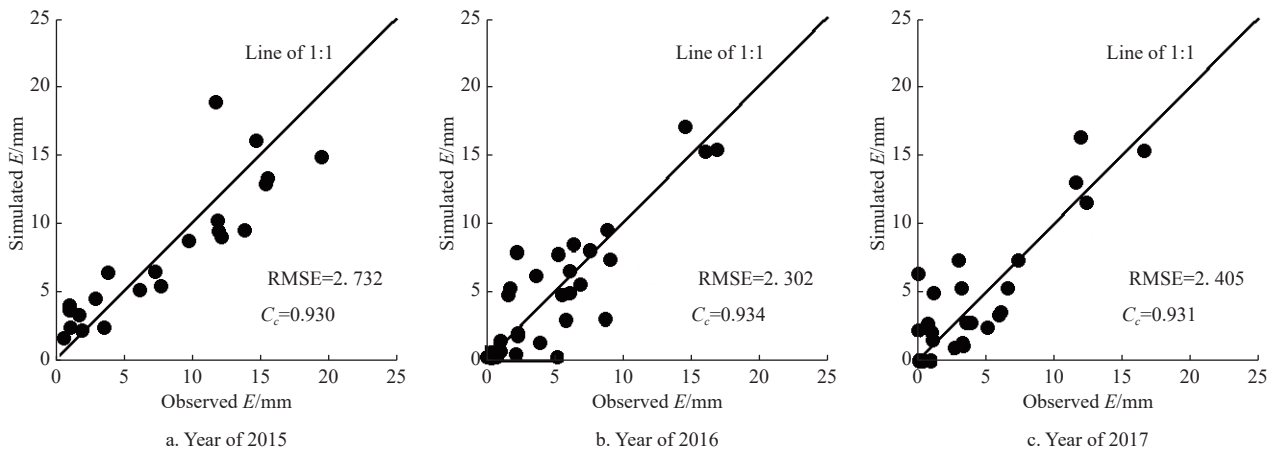
### 3.3 Model calibration and validation in typical grasslands

#### 3.3.1 Calibration and validation of vegetation coverage resistance

Based on the method described in section 2.3.3, measured  $E$  and related meteorological factors under the condition of soil moisture content exceeding the 60% field water capacity in 2015 and 2016 were used to calibrate the vegetation coverage resistance in three typical grasslands. Considering the obvious dynamics of vegetation coverage degrees during growing seasons, the calibration was carried out in each month, and the result was listed in Table 3. It can be seen that vegetation coverage resistances were distributed from 533.4-746.5, 767.4-1154.7, and 133.4-1334.5 s/m in the *I. cylindrica*, *M. sativa*, and *P. giganteum* plots, respectively. Specific values in three grasslands all showed a unimodal characteristic during growing seasons, and reached the maximum value in July in

the *I. cylindrica* and *M. sativa* plots, and August in the *P. giganteum* plot, respectively. Overall, variations of vegetation coverage resistances were larger in the *M. sativa* and *P. giganteum* plots than in the *I. cylindrica* plot, indicating that planted grass species are more likely to increase the uneven distribution of *E* during growing

seasons. When compared with *I. cylindrica*, *M. sativa* increased vegetation coverage resistances in every month, while *P. giganteum* reduced it at the beginning of the growing season, but increased it in the middle and late growing seasons.



Note: As the observation intervals are not fixed (1-7 d), the soil evaporation used in the figures are the cumulative values during each observation period.

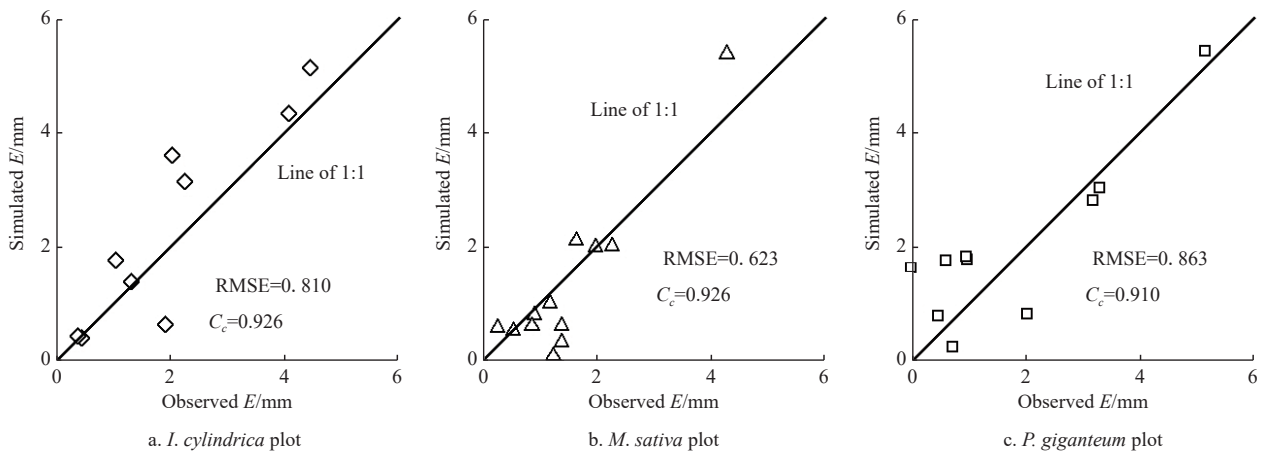
Figure 2 Comparison between observed and simulated soil evaporation in the bare land

**Table 3 Calculation results of vegetation coverage resistances in three typical grasslands**

Plots	Types	Apr	May	Jun	Jul	Aug	Sept	Oct
<i>I. cylindrica</i>	Natural grassland	533.4	580.4	674.1	746.5	733.5	699.1	567.4
<i>M. sativa</i>	Planted grassland	864.1	964.8	1042.4	1154.7	1065.7	933.1	767.4
<i>P. giganteum</i>	Planted grassland	133.4	388.9	961.5	1241.1	1334.5	1106.7	668.1

Note: The unit of data in the table is s/m.

Calibrated vegetation coverage resistances and field observations in 2017 were used to run the model, and the measured *E* was used to verify the reliability of the simulations (Figure 3). It was evident that the simulations fitted well with the observations, reaching low RMSE (0.810, 0.623, and 0.863 mm in the *I. cylindrica*, *M. sativa*, and *P. giganteum* plots, respectively) and high  $C_c$  (above 0.900 in all three plots). These values show good performances of the models, indicating that the calibrated vegetation coverage resistances are of acceptable accuracy and practicability.



Notes: As the observation intervals are not fixed (1-7 d), the soil evaporation used in the figures are the cumulative values during each observation period.

Figure 3 Validation results of vegetation coverage resistances in three typical grasslands

3.3.2 Calibration and validation of soil surface resistance

After validating vegetation coverage resistances, their values, together with measured *E* and related meteorological factors under conditions of soil moisture content lower than 60% field water capacity in 2015 and 2016 were used to calibrate soil surface resistances in three studied grasslands, and the results are shown as Figure 4. It can be found that soil surface resistances had ranges of 103.6-1610.2, 150.1-2405.3, and 105.7-1446.1 s/m in the *I. cylindrica*, *M. sativa*, and *P. giganteum* plots, respectively. All these resistances showed a decreasing trend with the increase of soil

moisture content, and their relationships could be expressed with three robust linear functions ( $p < 0.01$ ). It is noteworthy that the downward slopes of linear regressions in the *M. sativa* and *P. giganteum* plots were obviously lower than that in the *I. cylindrica* plot, showing that planted grasslands would make soil surface resistances change more rapidly with soil moisture. In terms of specific values, soil surface resistances were similar in the *I. cylindrica* and *P. giganteum* plots, and were considerably lower than that of the *M. sativa* plot, especially under lower soil moisture content, indicating that *M. sativa* is more conducive to preventing

the ineffective loss of soil water under dryer conditions.

Calibrated soil surface resistances, validated vegetation coverage resistances, and corresponding observations in 2017 were used to execute the model, and the measured  $E$  was used to test the accuracy of simulations (Figure 5). It can be seen that RMSE and  $C_c$  were 0.312 mm and 0.896, respectively, in the *M. sativa* plots, implying that simulated values were in better agreement with measured ones. It should be noted that  $E$  is inherently small when the soil moisture content is low, and at this time, just a small change

in  $E$  would have a great impact on the value of  $C_c$ . Therefore, although  $C_c$  in the *I. cylindrica* and *P. giganteum* plots was 0.762 and 0.789, respectively, and did not reach the good simulation threshold of 0.800, their RMSE was only 0.436 mm, which was still relatively low. Hence, it can also be considered that the validation results of soil surface resistances in the *I. cylindrica* and *P. giganteum* plots are still practical. To sum up, calibrated soil surface resistances in three plots could reasonably reflect the actual situation, and could be utilized to simulate  $E$  in all three plots.

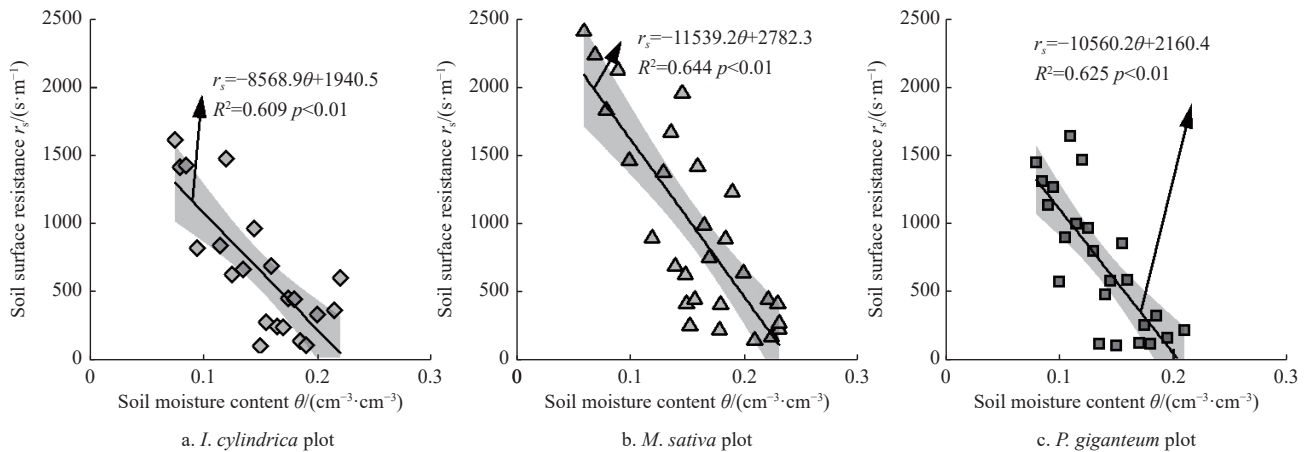
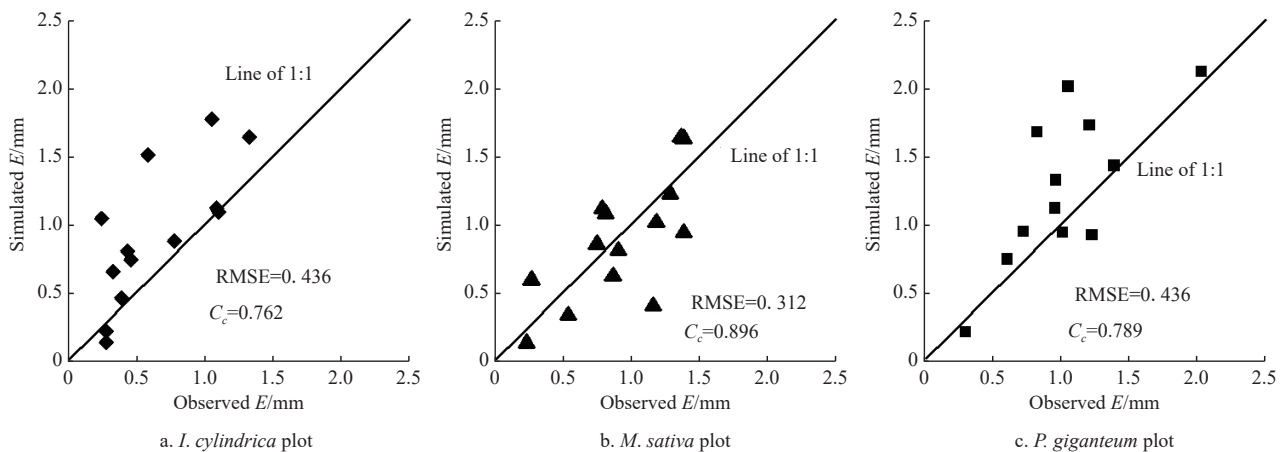


Figure 4 Relationships between soil surface resistances and soil moisture contents in three typical grasslands



Note: As the observation intervals are not fixed (1-7 d), the soil evaporation used in the figures are the cumulative values during each observation period.

Figure 5 Validation results of soil surface resistances in three typical grasslands

## 4 Discussion

### 4.1 Different stages of soil evaporation

The stages of soil evaporation are comprehensively influenced by multiple factors, such as soil moisture content, soil characteristics, meteorological factors, and vegetation conditions<sup>[2,32,33]</sup>. Numerous studies have shown that the variation of  $E$  with soil moisture content can be divided into three stages, namely the stage where  $E$  remains stable (the first stage), the stage where  $E$  increases with the moisture content (the second stage), and the water vapor diffusion stage where  $E$  is very small or does not exist (the third stage)<sup>[11,12,22]</sup>, and changes of soil water contents are the main reason why  $E$  is at different stages<sup>[6,26]</sup>. It is generally accepted that the soil moisture content threshold for the third and second stages is the wilting point<sup>[6,10]</sup>, while the split point for the second and first stages is the soil capillary rupture moisture content, and its value is close to 50%-80% field water capacity<sup>[6,11]</sup>. In this

study, the 60% field water capacity was selected as the threshold according to previous studies<sup>[11,22]</sup> and field observations, and based on this, the change of  $E$  also showed obvious phased characteristics (Figure 1). The results above were similar to numerous previous studies<sup>[6,15,22]</sup>, which further emphasized that the simulation model of  $E$  should have the ability to accurately reflect various characteristics of  $E$  at different stages.

In addition to the thresholds, an interesting phenomenon concerning relationships between  $E$  and soil moisture can also be seen in Figure 1:  $E$  and  $E/ET_0$  increased sharply with the improvement of soil moisture content in the second stage, and the upward slopes were considerably larger than those in numerous previous studies<sup>[11,12,22]</sup>, implying that when in this stage, a small increase of soil moisture would remarkably increase the amount of ineffective water loss in the studied grasslands. Such results also suggest the necessity and feasibility of adopting appropriate measures (e.g., vegetation and crop measures) to reduce ineffective

water loss through the regulation of soil moisture<sup>[26,34]</sup>.

#### 4.2 Soil surface resistance and vegetation coverage resistance

When  $E$  was in the second stage, the influence of moisture content on  $E$  was mainly reflected by the soil surface resistance. As the soil surface resistance was often not directly available, its relationships with soil moisture content had been widely investigated under various underlying conditions<sup>[28,35]</sup>. However, the change patterns of such research have been inconsistent; some studies reported nonlinear patterns, such as exponential<sup>[35]</sup> or power functions<sup>[27]</sup>, while others found linear relationships between them<sup>[22,28]</sup>, possibly due to the high heterogeneity in mulch types and soil conditions. Despite these change modes, soil surface resistances were all found to decrease with the increase of the soil moisture content in studies above<sup>[22,27,28,35]</sup>, which were similar to this study's results (Figure 4). When obtaining soil surface resistances, it is inevitably necessary to manually set the threshold of soil moisture content that divides  $E$  stages, which may cause errors in the simulations<sup>[2,22]</sup>. In this study, the threshold was selected as 60% of field water capacity. Based on this, this study derived that there were significant linear relationships ( $p < 0.01$ ) between soil surface resistance and soil moisture content in all three grasslands (Figure 4), which is consistent with many previous studies<sup>[22,28]</sup>. Validation results of these parameters showed that they can ideally reflect the actual situation of  $E$  processes (Figure 5), which in turn verified the correctness and practicability of the assumed soil moisture content thresholds in the three grasslands.

In addition to meteorological factors and soil moisture conditions, vegetation or crops will also markedly affect  $E$ . The vegetation canopy would alter the energy exchange process on the soil surface<sup>[7,8]</sup>. At the same time, root water absorption will also change the actual soil water potential<sup>[4,34]</sup>. The above effects may affect the resistance of water movement in the soil, and thereby cause changes in  $E$ . Therefore, the vegetation coverage resistance obtained in this study is a parameter reflecting the comprehensive influence of vegetation characteristics (leaf area, canopy thickness, root distribution, etc.). Considering that grass growth is highly dynamic<sup>[4,20]</sup>, the vegetation coverage resistances in the studied grasslands were not constant, but changed with the growth of grass (Table 2). Validation results of vegetation coverage resistances in all three grasslands showed that they can reasonably reflect the influence of different grass species on  $E$  (Figure 3), which also demonstrated the practical significance of encompassing various effects of vegetation into comprehensive resistance parameters to calculate  $E$ .

#### 4.3 Limitations and future outlook

In this study, the vegetation coverage resistance was proposed to facilitate the  $E$  simulation under vegetation conditions. Obviously, the vegetation coverage resistances are highly dynamic in different months and differ greatly among grasslands (Table 2), which is mainly because of the large differences in the physiological characteristics of grass species that can cause changes in soil surface radiation and soil water distribution<sup>[20,36]</sup>. However, how such characteristics influenced vegetation coverage resistances was not analyzed and discussed in the present study due to the lack of and difficulties in measuring them<sup>[36]</sup>. Apart from the vegetation factors, soil moisture content can also affect the calculation results of vegetation coverage resistances and soil surface resistances. In this study, soil moisture contents of surface soil were adopted for subsequent analysis based on the analysis of bare land (Figure 1) and other related studies<sup>[2,22]</sup>. However, several studies also showed that the use of soil moisture contents from other layers (layers 5 cm

or deeper) would also achieve better simulation results<sup>[3,9]</sup>, but this was not considered in this research. Furthermore, it should also be noted that the related soil physical properties (the saturated soil moisture content, field water capacity, etc.) were deemed to be unchanged during the experimental periods, and the validation results showed such an assumption was valid. Nevertheless, long-term vegetation restoration will inevitably cause changes in these properties<sup>[16]</sup>, and may ultimately affect vegetation coverage resistances and soil surface resistances<sup>[13]</sup>. The contents above may affect the simulation accuracy of  $E$  to a certain extent and should be taken into consideration in follow-up studies to improve the performance of the model, and to further deepen the understanding of the effect mechanisms of vegetation on  $E$ .

## 5 Conclusions

A three-year field experiment was conducted in a bare land, a natural grassland (*Imperata cylindrica* plot), and two planted grasslands (*Medicago sativa* and *Pennisetum giganteum* plots) in the semi-arid Loess Plateau to test the effectiveness of the basic form of the Van Bavel-Hillel model in soil evaporation simulation. The soil surface resistance and the newly proposed vegetation coverage resistance were calibrated and validated in three grasslands. The results revealed that the soil evaporation showed obvious stage characteristics with soil moisture, and 60% of field water capacity was effective as a threshold to divide the different stages of  $E$ . The basic form of the Van Bavel-Hillel model was effective to simulate the soil evaporation from bare land, and could be used to calculate the soil surface resistance and vegetation coverage resistance under vegetation conditions. Validated soil surface resistances and vegetation coverage resistances could reasonably reflect the actual situations of soil evaporation processes in studied grasslands. Soil surface resistances decreased linearly ( $p < 0.01$ ) with the increase of the soil moisture content in all three grasslands, and the decreasing rates were similar in *M. sativa* and *P. giganteum* plots, which were considerably higher than that in the *I. cylindrica* plot. Vegetation coverage resistances in the three plots all showed a unimodal characteristic during growing seasons. When compared with *I. cylindrica*, *M. sativa* increased the vegetation coverage resistance in every month, while *P. giganteum* reduced it at the beginning of the growing season, but increased it in the middle and late growing season.

This study shows that it is feasible to use the vegetation coverage resistances to comprehensively reflect the influence of vegetation, providing a new perspective for the calculation of soil evaporation in semi-arid ecosystems. In addition, obtained vegetation coverage resistances and soil surface resistances in three typical grasslands can also provide practical references for grass species selection and water resources management in the vegetation restoration of the Loess Plateau.

## Acknowledgements

This research was financially supported by the Natural Science Basic Research Plan in Shaanxi Province of China (Grant No. 2023-JC-ZD-30 and 2019JZ-45), the National Natural Science Foundation of China (Grant No. 42301047, 41771259 and 41171034), the Shaanxi Provincial Water Conservancy Science and Technology Project (Grant No. 2016slkj-11), and the Shaanxi Provincial Key Laboratory Project of Department of Education (Grant No. 14JS059).

**[References]**

- [1] Or D, Lehmann P, Shahraeeni E, Shokri N. Advances in soil evaporation physics - A review. *Vadose Zone Journal*, 2013; 12(4): 1–16.
- [2] Bittelli M, Ventura F, Campbell G S, Snyder R L, Gallegati F, Pisa P R. Coupling of heat, water vapor, and liquid water fluxes to compute evaporation in bare soils. *Journal of Hydrology*, 2008; 362(3–4): 191–205.
- [3] Ponciano I M, Miranda J H, Santos M A, de Jong van Lier Q, Grah V F. An empiric model for predicting soil daily evaporations: soil and atmospheric variables. *Revista Brasileira de Agricultura Irrigada*, 2015; 9(4): 225–231.
- [4] Zhao X K, Song X Y, Li L J, Wang D Y, Meng P F, Li H Y. Effect of microrelief features of tillage methods under different rainfall intensities on runoff and soil erosion in slopes. *International Soil and Water Conservation Research*, 2024; 12(2): 351–364.
- [5] Jiao L, Lu N, Fu B J, Wang J, Li Z S, Fang W W, et al. Evapotranspiration partitioning and its implications for plant water use strategy: Evidence from a black locust plantation in the semi-arid Loess Plateau, China. *Forest Ecology and Management*, 2018; 424: 428–438.
- [6] Seneviratne S I, Corti T, Davin E L, Hirschi M, Jaeger E B, Lehner I, et al. Investigating soil moisture-climate interactions in a changing climate: A review. *Earth-Science Reviews*, 2010; 99(3–4): 125–161.
- [7] Yan H F, Zhang C, Hiroki O, Peng G J, Ransford O D. Determination of crop and soil evaporation coefficients for estimating evapotranspiration in a paddy field. *Int J Agric & Biol Eng*, 2017; 10(4): 130–139.
- [8] White M A, Thornton P E, Running S W, Nemani R R. Parameterization and sensitivity analysis of the BIOME-BGC terrestrial ecosystem model: net primary production controls. *Earth interactions*, 2000; 4(3): 1–85.
- [9] Allen R G, Pereira L S, Raes D, Smith M. FAO Penman-Monteith equation. Allen R G, Pereira L S, Raes D, Smith M (Ed.). *Crop evapotranspiration: Guidelines for computing crop requirements*. Rome, Italy: FAO, 1998; pp.17–23.
- [10] Sun S J, Fan Y M, Liu Y P, Zhang X D, Xu Z H, Chi D C. Measurement and influencing factors of soil evaporation between plants. *Water Saving Irrigation*, 2014; 4: 79–82. (in Chinese)
- [11] Jiang J M. Research on the evaporation and transpiration models of soil. *Journal of Sichuan Forestry Science and Technology*, 1995; 16(4): 20–25. (in Chinese)
- [12] Sun J S, Kang S Z, Wang J L, Li X D, Song N. Experiment on soil evaporation of summer maize under furrow irrigation condition. *Transactions of the CSAE*, 2005; 21(11): 20–24. (in Chinese)
- [13] Wang Y Q, Merlin O, Zhu G F, Zhang K. A physically based method for soil evaporation estimation by revisiting the soil drying process. *Water Resources Research*, 2019; 55(11): 9092–9110.
- [14] Wu Y J, Du T S. Evaporation and its influencing factors in farmland soil in the arid region of Northwest China. *Transactions of the CSAE*, 2020; 36(12): 110–116. (in Chinese)
- [15] Koster R D, Dirmeyer P A, Guo Z C, Bonan G, Chan E, Cox P, et al. Regions of strong coupling between soil moisture and precipitation. *Science*, 2004; 305(5687): 1138–1140.
- [16] Guo M M, Wang W L, Kang H L, Yang B. Changes in soil properties and erodibility of gully heads induced by vegetation restoration on the Loess Plateau, China. *Journal of Arid Land*, 2018; 10(5): 712–725.
- [17] Feng X M, Fu B J, Piao S L, Wang S, Ciais P, Zeng Z Z, et al. Revegetation in China's Loess Plateau is approaching sustainable water resource limits. *Nature Climate Change*, 2016; 6(11): 1019–1022.
- [18] Wu G L, Liu Y F, Cui Z, Liu Y, Shi Z H, Yin R, et al. Trade-off between vegetation type, soil erosion control and surface water in global semi-arid regions: A meta-analysis. *Journal of Applied Ecology*, 2020; 57(5): 875–885.
- [19] Li L J, Song X Y, Xia L, Fu N, Li H Y, Li Y L, et al. Response of evaporation and transpiration of typical afforestation tree species to climate changes in gully region of Loess Plateau. *Transactions of the CSAE*, 2018; 34(20): 148–159. (in Chinese)
- [20] Ryu Y, Baldocchi D D, Ma S Y, Hehn T. Interannual variability of evapotranspiration and energy exchange over an annual grassland in California. *Journal of Geophysical Research*, 2008; 113. doi: [10.1029/2007JD009263](https://doi.org/10.1029/2007JD009263).
- [21] Li L J, Song X Y, Xia L, Fu N, Feng D, Li H Y, et al. Modelling the effects of climate change on transpiration and evaporation in natural and constructed grasslands in the semi-arid Loess Plateau, China. *Agriculture, Ecosystems & Environment*, 2020; 302: 107077.
- [22] Li Y, Liu H J, Huang G H. Modeling resistance of soil evaporation and soil evaporation under straw mulching. *Transactions of the CSAE*, 2015; 31(1): 98–106. (in Chinese)
- [23] van Genuchten M T. A closed-form equation for predicting the hydraulic conductivity of unsaturated soils. *Soil Science Society of American Journal*, 1980; 44(5): 892–898.
- [24] Mualem Y. A new model for predicting the hydraulic conductivity of unsaturated porous media. *Water Resources Research*, 1976; 12(3): 513–522.
- [25] van Bavel C H M, Hillel D I. Calculating potential and actual evaporation from a bare soil surface by simulation of concurrent flow of water and heat. *Agricultural Meteorology*, 1976; 17(6): 453–476.
- [26] Qiu Y, Xie Z K, Wang Y J, Ren J L, Malhi S S. Influence of gravel mulch stratum thickness and gravel grain size on evaporation resistance. *Journal of Hydrology*, 2014; 519: 1908–1913.
- [27] Sun S F. Moisture and heat transport in a soil layer forced by atmospheric conditions. Master dissertation. Connecticut, The United States of America: University of Connecticut, 1982; 41p.
- [28] Camillo P J, Gurney R J. A resistance parameter for bare-soil evaporation models. *Soil Science*, 1986; 141(2): 95–105.
- [29] Fu N, Song X Y, Xia L, Li L J, Li H Y, Li Y L. Complementary relationship and dual crop coefficient approach-based study on green water separation. *Water*, 2019; 11(2): 378.
- [30] Zeppetello L R V, Battisti D S, Baker M B. The origin of soil moisture evaporation "Regimes". *Journal of Climate*, 2019; 32(20): 6939–6960.
- [31] Wang Y S, Zhang Y G, Yu X X, Jia G D, Liu Z Q, Sun L B, et al. Grassland soil moisture fluctuation and its relationship with evapotranspiration. *Ecological Indicators*, 2021; 131: 108196.
- [32] Merz S, Pohlmeier A, Vanderborgh J, van Dusschoten D, Vereecken H. Moisture profiles of the upper soil layer during evaporation monitored by NMR. *Water Resources Research*, 2014; 50(6): 5184–5195.
- [33] Feng W Y, Wang T K, Yang F, Cen R, Liao H Q, Qu, Z Y. Effects of biochar on soil evaporation and moisture content and the associated mechanisms. *Environmental Science Europe*, 2023; 35: 66.
- [34] Guo X H, Lei T, Sun X H, Ma J J, Zheng L J, Zhang S W, et al. Modelling soil water dynamics and root water uptake for apple trees under water storage pit irrigation. *Int J Agric & Biol Eng*, 2019; 12(5): 126–134.
- [35] van de Griend A A, Owe M. Bare soil surface resistance to evaporation by vapor diffusion under semiarid conditions. *Water Resources Research*, 1994; 30(2): 181–188.
- [36] Liu H J, Gao Z Z, Zhang L W, Liu Y. Stomatal conductivity, canopy temperature and evapotranspiration of maize (*Zea mays* L.) to water stress in Northeast China. *Int J Agric & Biol Eng*, 2021; 14(2): 112–119.